Journal of Hazardous Materials 448 (2023) 130877

Contents lists available at ScienceDirect

Journal of Hazardous Materials

journal homepage: www.elsevier.com/locate/jhazmat

Research Paper

Multiple mechanisms collectively mediate tungsten homeostasis and resistance in *Citrobacter* sp. Lzp2

Zipei Luo [a], Zhen Li [b], Jing Sun [c], Kaixiang Shi [d], Ming Lei [a], Boqing Tie [a], Huihui Du [a,*]

[a] College of Resources and Environment, Hunan Agricultural University, 410127 Changsha, China
[b] College of Resources and Environmental Sciences, Nanjing Agricultural University, 210095 Nanjing, China
[c] State Key Laboratory of Environmental Geochemistry, Institute of Geochemistry, Chinese Academy of Sciences, 550081 Guiyang, China
[d] State Key Laboratory of Agricultural Microbiology, College of Life Science and Technology, Huazhong Agricultural University, 430070 Wuhan, China

HIGHLIGHTS

- A whole W-resistance mechanism network was constructed for *Citrobacter* sp. Lzp2.
- W induces the secretion of extracellular protein to chelate W via the carboxylic groups.
- Tetrathionate respiration is a potential metabolic pathway to detoxicating W.
- Chaperone protein and metal-binding pterin are important reservoirs of intracellular W.
- *Citrobacter* sp. Lzp2 has a high potential in W's bio-recovery and bioremediation.

GRAPHICAL ABSTRACT

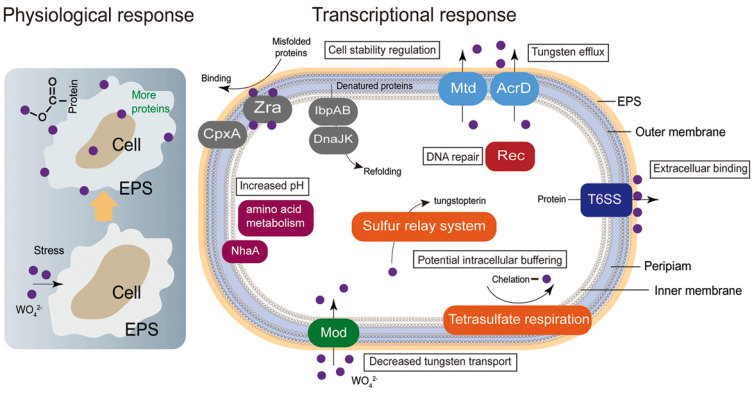

ARTICLE INFO

Editor: Dr. R. Debora

Keywords:
Tungsten
Microorganism
Resistance
Homeostasis
Transcriptome

ABSTRACT

Tungsten (W) is an emerging contaminant, and current knowledge on W resistance profiles of microorganisms remains scarce and fragmentary. This study aimed to explore the physiological responses of bacteria under W stress and to resolve genes and metabolic pathways involved in W resistance using a transcriptome expression profiling assay. The results showed that the bacterium *Citrobacter* sp. Lzp2, screened from W-contaminated soil, could tolerate hundreds of mM W(VI) with a 50% inhibiting concentration of ~110 mM. To cope with W stress, *Citrobacter* sp. Lzp2 secreted large amounts of proteins through the type VI secretory system (T6SS) to chelate W oxoanions via carboxylic groups in extracellular polymeric substances (EPS), and could transport cytosolic W outside via the multidrug efflux pumps (*mdtABC* and *acrD*). Intracellular W is probably bound by chaperone proteins and metal-binding pterin (tungstopterin) through the sulfur relay system. We propose that tetrathionate respiration is a new metabolic pathway for cellular W detoxification likely producing thio-tungstate. We conclude that multiple mechanisms collectively mediate W homeostasis and resistance in *Citrobacter* sp. Lzp2. Our results have important implications not only for understanding the intricate regulatory network of W homeostasis in microbes but also for bio-recovery and bioremediation of W in contaminated environments.

* Corresponding author.
E-mail address: duhuihui@hunau.edu.cn (H. Du).

https://doi.org/10.1016/j.jhazmat.2023.130877
Received 1 November 2022; Received in revised form 19 January 2023; Accepted 25 January 2023
Available online 26 January 2023

1. Introduction

Tungsten (W) is a transition metal and has been widely used in industrial and life applications due to its high melting point, high hardness, and stable chemical properties [1,2]. In tungsten mine- and munition-impacted regions, high W accumulation has been found in soils [3,4], sediments [5], atmosphere [6], surface- [7,8], and ground-waters [9]. Therefore, the exposure of biosphere to elevated levels of W is increasing. Although W was presumed as a non-toxic metal, more recent research has shown that chronic high W exposure could inhibit plant root's nitrate reductase activity [10], shift soil microbial community [11], induce reproductive toxicity to earthworm [12], and even potentially cause childhood leukemia [13]. The United States Environmental Protection Agency (EPA), therefore, has classified W as an emerging contaminant [14]. However, the potential threat of W to the biosphere remains poorly characterized.

Microorganisms are a major component of Earth's biosphere, which are widely distributed in the environment and highly sensitive to ambient stress [15,16]. Indeed, there are mounting evidences that W is toxic to microbes. For example, 0.1 mM tungstate resulted in a ~80% reduction in the growth rate of *Azotobacter vinelandii*, a nitrogen-fixing bacterium [17]. Tungstate was also found to inhibit the growth of *Pseudomonas fluorescens* and *Bacillus subtilis* [18], and iron-oxidizing bacteria *Acidithiobacillus ferrooxidans* [19]. Such adverse effects on the survival, metabolism, and reproduction of microbes would significantly jeopardize their biological functions. The elucidation of the biological effects of W on microorganisms and how microbes cope with W stress is key to understanding not only its threat to Earth's biosphere and environmental safety but also the controls that can reduce its ecological risk.

To cope with elevated concentrations of toxic substances, microorganisms can evolve different and yet complementary resistance mechanisms including extracellular barrier, reduced uptake, active transport (efflux), intracellular accumulation, and oxidation/reduction [15,16,20,21-23]. Although relatively rare, using real-time polymerase chain reactions (real-time PCR), experimental evidence showed efflux is an important metabolic process for intracellular W homeostasis. For example, Leblanc et al. [24] argued that tungstate induced the upregulated expression of the BaeSR system in *Escherichia coli*, which commonly participates in bacterial drug resistance and efflux. A tungstate response regulator familiar *tunR* including genes *modABC* and toluene sulfonate uptake family transporters can control tungstate homeostasis by regulating efflux or uptake of a substance to overcome the inhibiting effect of W in sulfate-reducing bacteria [25]. Moreover, extracellular sequestration of W by catechol siderophores has been considered important for *A. vinelandii* to satisfy its molybdenum (Mo) requirement and avoid W toxicity [17]. These preliminary investigations only tested known resistance genes and metabolic pathways that have been postulated importantly for other toxic metals. Nevertheless, many fundamental questions such as how W is bound to extracellular components determines how readily W can be transported into the cells, and how bacteria storage and detoxicate intracellular W, remain unclear.

High-throughput transcriptome sequencing (RNA-seq) offers a practicable way to understand the biological responses of bacteria under metal stress from the whole transcriptional level. By using RNA-seq, Huang et al. [26] argued that multiple systems including sulfur metabolism, iron-sulfur, and cell secretion are involved in mediating copper (Cu) resistance in strain *Cupriavidus gilardii* CR3, in addition to revealing known Cu resistance-related genes. For cadmium (Cd), efflux from the cytoplasm, biofilm formation enabling absorption, histidine metabolism, and flagellar assembly collectively regulated Cd resistance in *Pseudomonas chenduensis* strain MBR [27]. We postulate that RNA-seq may help to unravel the metabolic pathways that are responsible for the uptake, efflux, buffering, and detoxification of W, and to construct a whole W resistance network.

The main objective of this study was to obtain a first W resistance profile using a combination of physiological and transcriptomic approaches. We used *Citrobacter* sp. Lzp2, which was screened from W-contaminated soil near an abandoned tungsten smelter, as a model bacterium. Previous studies have shown *Citrobacter* strains can tolerate various heavy metals, including mercury, cadmium, and chromium, through multiple mechanisms, and could adsorb large amounts of heavy metals [28,29]. We examined their physiological changes under different W stresses through analysis of growth curves, extracellular secretion, and morphology. Accumulation characteristics including intracellular versus extracellular contributions, chelation/complexation mechanisms, and valence states were systematically studied. Additionally, RNA-seq was employed to elucidate the resistance mechanisms at the transcriptome level. The macro and molecular mechanisms are organically combined to form a complete and thorough resistance mechanism network, which is vital not only for advancing the ecotoxicology profiles of W but also for a better understanding of how resistant bacteria can be exploited for efficient bioremediation of W-contaminated environments.

2. Materials and methods

2.1. W-resistant bacteria isolation and identification

The W-resistant bacteria were screened from W-contaminated soil (~3190 mg/kg) near an abandoned W smelter in Xiangdong Tungsten Mine area, Chaling City, China (27°2′0.96″N, 113°47′44″E), which is one of the largest W-mine in China and was exploited for more than 100 years before its closure. Detailed site description, soil properties, and tungsten geochemical profiles can be found in a previous study [30]. Ten grams of soil was first mixed with 200 mL sterile deionized water and shaken at 30 °C for 30 min. A 1-mL aliquot of the suspension was transferred to a Luria-Bertani (LB) medium (Tryptone 10 g/L, yeast extract 5 g/L, and NaCl 5 g/L, pH ~6.8) containing 5 mM of W, added as Na_2WO_4, and incubated for 2 days. The bacterial solutions were then diluted sequentially with a series of LB medium containing up to 30 mM W for selective screening of W-resistant bacteria. The culture solution was spread onto LB agar media containing 30 mM W and incubated at 30 °C for 2 days. A fast-growing single colony was selected and purified for the following experiments.

To identify the isolated bacterium, DNA was extracted and 16 S rRNA genes were PCR-amplified using the bacterial universal primers 27 f (5′-AGA GTT TGA TCC TGG CTC AG-3′) and 1492r (5′-GGC TAC CTT GTT ACG ACT T-3′) by Hangzhou Lianchuan Biotechnology Co. LTD, and analyzed by BLAST (http://blast.ncbi.nlm.nih.gov/Blast.cgi). Based on the phylogenetic trees constructed with MEGA7.0, and evolutionary distances analyses (Fig. S1), the isolated bacterium belongs to *Citrobacter* sp., named *Citrobacter* sp. Lzp2 and deposited in the GenBank (accession number: MW012678).

2.2. Bacterial growth curve, extracellular secretion, and cell morphology,

Growth curve for *Citrobacter* sp. Lzp2 was performed by culturing cells in an LB medium supplemented with different concentrations of W ranging between 0 and 180 mM at 30 °C until the stable growth stage was reached. Each treatment was prepared in triplicate. The commonly used biomass indicator, optical density at 600 nm (OD_{600}), was recorded using a UV–visible spectrophotometer, and growth curves were constructed as time versus OD_{600} values. Cells under different treatments (0, 35, 70, and 110 mM W) were collected at the stable growth stage (~90 h). A one-way analysis of variance (ANOVA) was carried out to check for statistical differences between different groups using the SPSS package. The *P* value was set at 0.05 for significant differences.

To quantify the composition of extracellular secretions, total extracellular polymeric substances (EPS) were first extracted using a heating method reported in Teng et al. [31]. The polysaccharide of EPS was then measured by the anthrone method [32]. Reagent: a 0.1% solution of anthrone was made up in 80% (v/v) H_2SO_4 before use. Standards: a

series of glucose solutions (0–100 mg/L). Procedures: 1 mL EPS samples were mixed with 1 mL reagent in a digestion tube, then placed in a water bath at 100 °C for 14 min, and then refrigerated in a water bath at 5 °C for 5 min. The samples and standards were measured spectrophotometrically at 625 nm. The protein of EPS was determined using the Bradford method [33]. Reagent: 0.1 g coomassie blue was dissolved in 50 mL 95% ethanol, then 100 mL 85% (w/v) H_3PO_4 was subsequently added and finally diluted to 1 L using distilled water. Standards: a series of bovine serum albumin (BSA) solutions (0–100 μg/L). Procedures: 0.2 mL EPS samples were mixed with 5 mL reagent, and allowed to react for 20 min. The samples and standards were measured spectrophotometrically at 595 nm.

Fourier transform infrared spectroscopy (FTIR) was supplemented to semi-quantitatively determine EPS composition. During FTIR measurement, each spectrum was collected in the range of 4000–600 cm^{-1} at a resolution of 4 cm^{-1}. A proportion of the harvested cells were fixed in 2.5% glutaraldehyde, then subjected to an ethanol dehydration series and freeze-dried for determination of cell morphology using scanning electron microscopy (SEM, Quanta F250, Germany). The cell-size distribution was analyzed using Software Nano Measurer [34].

2.3. Intracellular and extracellular W determination

Different types of extractants have been used to separate the cell surface-adsorbed metal(loids), such as EDTA for Cu and Cd [26,35], and PO_4^{3-} for As [36]. However, there is no readily available method for the determination of surface-adsorbed W. Since W exists mainly as oxoanions, it is reasonable to use other oxoanions to desorb W from the adsorption sites. Gustafsson, [37] showed that phosphate did not affect WO_4^{2-} adsorption on ferrihydrite at pH< 5, but significantly inhibited WO_4^{2-} adsorption at pH> 7. Based on this characteristic, 0.1 M phosphate buffer solution at pH 7.0 was used as a tentative agent to extract the cell surface-bound W. The harvested cells at the stable growth stage were first washed three times with deionized water and re-suspended in a 0.1 M phosphate buffer solution. The mixed solution was agitated at 150 rpm for 30 min. After centrifuging at 10,000 g for 5 min, the supernatant was retained for determining the extracellular W, and the remained cell pellets were freeze-dried and subject to acid digestion (70% nitric acid) to measure the intracellular W. The concentrations of W in the extracts were determined by Inductively Coupled Plasma Optical Emission Spectrometer (ICP-OES, PerkinElmer Optima 8300) following the procedures in Du et al., [30]. Tungsten 4 f XPS was used to examine the change of the W valence state. The samples were analyzed on a KRATOS Axis Ultra X-ray photoelectron spectrometer (Thermo Fisher Scientific, USA). FTIR was used to obtain the changes in functional groups before and after W exposure.

2.4. Transcriptome sequencing and data analyses

Transcriptome experiments were performed by selecting two W concentrations based on the growth curves: a slightly inhibitory concentration, 35 mM, and a highly inhibitory concentration, 70 mM. W-free blank (0 mM) served as the control. *Citrobacter* sp. Lzp2 was cultivated in an LB medium to an OD_{600} value of 1 and then exposed to these three different W concentrations. Three biological repeats were carried out for each treatment. Cells were centrifugally collected at the logarithmic growth phase and sent for RNA extraction, reverse transcription, and transcriptome sequencing to the Shanghai Majorbio Bio-pharm Technology Co., Ltd. To select the high-quality different genes, the original sequence data were first analyzed, filtered, and compared with the specified reference genome. The different genes were selected based on selecting conditions, a false discovery rate (FDR) ≤ 0.05 and $|\log FC| \geq 1$, which means $p \leq 0.05$, and the difference multiple exceeding 2. Raw reads were deposited to the NCBI Sequence Read Archive with the accession number SRP386990.

According to phylogenetic analysis based on 16 S rRNA, *Citrobacter* sp. Lzp2 showed high homology (higher than 99% identity) with many *Citrobacter* strains in the public database (Fig. S1). In this study, whole-genome sequence of *Citrobacter farmeri* AUSMDU00008141 (accession number: CP022695) was used for transcriptome annotation analysis. The Gene Ontology (GO) database was used to classify the functions of different genes, and GOATOOLS was used to perform the GO enrichment analysis. R-script was used for Kyoto Encyclopedia of Genes and Genomes (KEGG) PATHWAY enrichment analysis. The enrichments of GO and KEGG PATHWAY functions were analyzed through Fisher's accurate test and *p*-value correction (BH (FDR) method), where corrected *p* values (*p*-adjust)< 0.05 indicated significant enrichment.

2.5. qRT-PCR

To validate the RNA-seq results, qRT-PCR was performed on a StepOne™ Real-Time PCR system using TransStart Top Green qPCR SuperMix (TransGen). The special primers and the randomly selected eight genes for qRT-PCR are listed in Table S1. Gene transcript levels were normalized to 23 S rRNA by the $2^{-\Delta\Delta Cq}$ approach [38].

3. Results

3.1. W affected bacterial growth, reduced cell size, and induced protein secretion

While cell growth was not affected at W concentration < 5 mM, slight but not significant ($p > 0.05$) differences were observed in OD_{600} values when the W concentration was raised to 35 mM (Fig. 1 A). The bacterial biomass was decreased significantly ($p < 0.05$) at > 55 mM W, and reduced to half of the maximum biomass at ~110 mM W. *Citrobacter* sp. Lzp2 strain shows a huge resistance to W compared to other bacterial strains reported in previous studies (Table S2).

In the absence of W (control), *Citrobacter* sp. Lzp2 cells are short rod-shaped with an average cell length of ~738 ± 100 nm (Fig. 1B-E and S2). Compared to the control, the cell body sizes were reduced by ~11%, 22%, and 27% at 35, 70, and 110 mM W, respectively. More cellular collapses were observed at > 70 mM W.

The total extracellular polysaccharide fraction barely changed, whereas the protein fraction increased with increasing W concentration from 0 to 110 mM (Fig. 1 F). Correspondingly, the ratio of polysaccharide/protein declined from 0.64 to 0.23. The normalized FTIR absorption peaks for the protein fraction (amide I at ~1650 cm^{-1} and amide II at ~1549 cm^{-1}) increased, whereas those for the polysaccharide fraction remained unchanged (Fig. S3A and B). Peak area results further revealed a decreased polysaccharide/protein ratio with increasing W concentrations (Fig. S3B). These observations suggested that *Citrobacter* sp. Lzp2 secreted more protein to cope with W stress.

3.2. W biological enrichment characteristics

As the W concentration increased from 35 to 110 mM, extracellular biosorption increased from 1.1 ± 0.39–3.3 ± 0.78 mmol/g and intracellular bioaccumulation increased from 0.5 ± 0.04–1.7 ± 0.16 mmol/g (Fig. 2 A). Extracellular biosorption was significantly greater than those of intracellular bioaccumulation ($p < 0.05$), with a measured intercellular to extracellular ratio between 0.318 and 0.515. The actual ratio could be even larger assuming PO_4^{3-} could not completely desorb W from the bacterial cell surface. Overall, extracellular biosorption was dominant for *Citrobacter* sp. Lzp2 to accumulate W.

FTIR identified the carboxylic (~1397 cm^{-1}) and phosphate (~1236 cm^{-1}) groups on cell surfaces (Fig. 2B). The peak intensity of the COO^- decreased significantly and shifted to a lower frequency (~1397 cm^{-1}), implying the carboxylic sites were responsible for the binding of W, probably via chelation/complexation. The new absorption peaks at ~894 and 962 cm^{-1} for W-loaded *Citrobacter* sp. Lzp2 represented the symmetric stretching vibration of W–O vibrations [39].

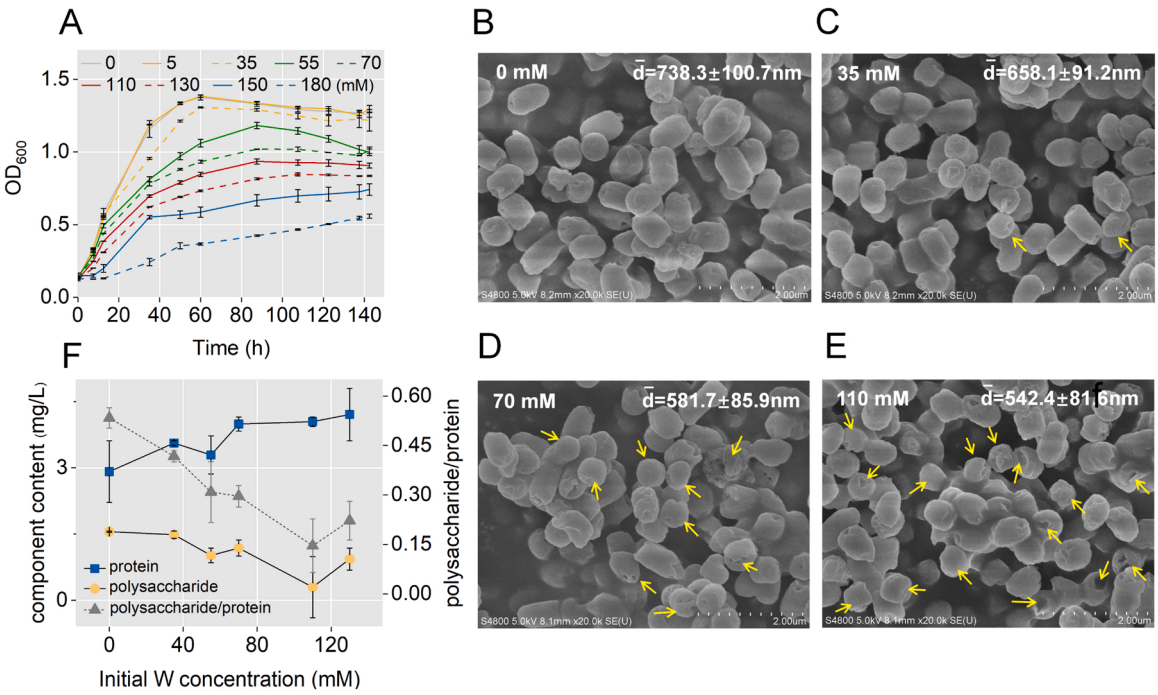

Fig. 1. Effects of W on bacterial growth and morphology, and EPS chemical composition. A. Growth curves for bacterium *Citrobacter* sp. Lzp2 in LB medium treated with different W concentrations (0, 5, 35, 55, 70, 110, 130, 150, 180 mM) at 30 °C. Data are plotted as optical density at 600 nm (OD_{600}) versus time (h). B-E. Scanning electron micrographs of *Citrobacter* sp. Lzp2 cells at the stable growth stage under the stress of different W (0, 35, 70, and 110 mM). The averaged diameter size ($\bar{d}$) was calculated based on > 30 cells (see Fig. S2). The yellow arrows point to the cells' collapse. F. Analyses of total extracellular polymeric substances (EPS): The left *y*-axis represents the protein (blue dots) and polysaccharide (yellow dots) content in the presence of different W (0, 35, 55, 70, 110, and 130 mM), while the right *y*-axis represents the ratio of polysaccharides to proteins (gray dotted line). For growth curves (A) and EPS analyses (F), error bars represent standard errors of three biological replicates.

According to XPS (Fig. 2 C and D), the valence state of cell-bound W remained +VI during W accumulation on *Citrobacter* sp. Lzp2.

3.3. Distribution of differentially expressed genes and qRT-PCR validation

In total, 191 million clean reads were obtained, with 94.2–97.34% of them successfully mapped to the reference genome (Table S3). Principal component analysis and hierarchical clustering showed good parallel correlations and significant differences for each set (Fig. 3 A and B). In comparison with the control (0 mM W), 209 differential genes (62 upregulated and 147 downregulated) and 381 differential genes (162 upregulated and 219 downregulated) were significantly expressed by 35 mM and 70 mM W, respectively (Fig. 3 C). There were 57 differential expressed genes (20 upregulated and 37 downregulated) between the 35 mM and 70 mM W treatments (Fig. 3 C), suggesting several different responses under different W treatments.

To validate the RNA-seq results, eight differentially expressed genes (5 upregulated and 3 downregulated) were randomly selected and conducted for qRT-PCR analysis (Fig. 3D and Table S4). Regulatory trends were consistent with RNA-seq and the correlation between qRT-PCR and RNA-seq data was significant (R^2=0.861, $p < 0.001$).

3.4. GO and KEGG enrichment analysis of differentially expressed genes

To explore the functional differences in differentially expressed genes, the biological functions in GO term were classified into three categories: cellular component (CC), molecular function (MF), and biological process (BP) (Fig. 4). In general, the GO terms were mainly enriched ($p < 0.05$) in BP and MF under W stress. Towards the upregulated genes, 18 and 19 GO terms were enriched at 35 mM and 70 mM W, respectively (Fig. 4A). In the presence of 35 mM W, amino acid metabolism-related processes including histidine catabolic (GO:0006548), glutamate metabolic (GO:0006536), dicarboxylic acid catabolic (GO:0043649), and alpha-amino acid catabolic (GO:1901606) processes were activated. In the presence of 70 mM W, the most significantly enriched GO items were annotated as coding for proteins involved in cell stabilization such as unfolded protein binding (GO:0051082), protein folding (GO:0006457), DNA replication (GO:0006260), and cation homeostasis (GO:0055080). Molybdopterin cofactor binding (GO:0043546) and regulation of pH (GO:0006885) were both overexpressed under the two treatments. Overall, W exposure induced the overexpression of genes involved in amino acid and protein metabolism, cell stability regulation, molybdopterin cofactor binding, and regulation of pH.

Towards the downregulated genes (Fig. 4B), 21 and 19 GO terms were significantly enriched by the presence of 35 mM and 70 mM W, respectively, including cell motility (GO: 0006935, 0040011, 0001539, and 0048870), energy metabolism (GO:0052646, 0009401, and 0006040), and response to oxidative activity (GO: 0016651, 0004601, 0006979, and 0016209). These underexpressed genes indicated the increase of oxidative stress and decrease of movement and energy metabolism of *Citrobacter* sp. Lzp2.

Three pathways were significantly enriched by upregulated genes under the stress with 35 mM W, i.e., the two-component system (map02020), sulfur metabolism (map00920), and the sulfur relay system (map04122) (*p*-adj<0.05) (Fig. 5). The two-component system was also enriched significantly under 70 mM W (*p*-adj<0.05), while the sulfur metabolism and sulfur relay system were enriched with significantly uncorrected *p*-values ($p < 0.05$). Therefore, different W stresses induced similar transcriptional responses in *Citrobacter* sp. Lzp2. Notably, all upregulated genes in the secretory system were enriched in the bacterial secretion system (Type VI, T6SS) (map03070) at 70 mM W (Fig. 5). Pathways involved in the phosphotransferase system

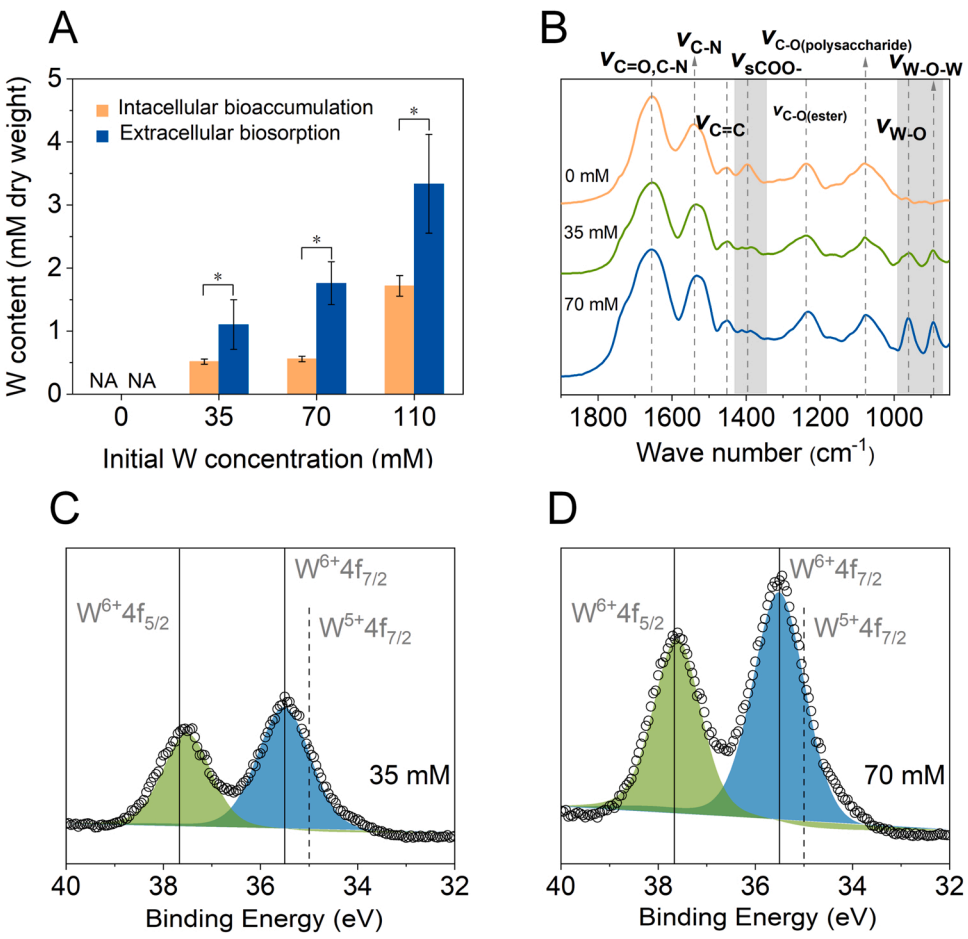

Fig. 2. W biological enrichment characteristics. A. Intracellular and extracellular W enrichment (mM/dry weight cells) for *Citrobacter* sp. Lzp2 exposing to different W (0, 35, 70, 110 mM) at the stable growth stage. NA: not available. Error bars are standard errors of three biological replicates. *represents a significant difference ($p < 0.05$) between the intracellular and extracellular W amounts. B. Fourier transform infrared (FT-IR) spectra and C, D. XPS spectra of *Citrobacter* sp. Lzp2 cells under different W concentrations.

(map02060), pyruvate metabolism (map00620), pentose phosphate pathway (map00030), glycerophospholipid metabolism (map00564), and bacterial chemotaxis (map02030) were significantly enriched by downregulated genes, indicating that the energy metabolism of *Citrobacter* sp. Lzp2 was inhibited.

Based on GO and KEGG enrichment results, metabolic pathways associated with protein metabolism, cell stability regulation, bacterial secretion, two-component system, and sulfur relay system play a key role in W-resistance (Fig. 6). Genes linked to protein metabolism are mainly *astBED*, *hutGHIU*, *glmES*, *argC*, and *putA* (Table S5). Genes *ibpAB, groL*, *htpG*, *dnaJK*, *clpB*, *cpxP,* and *fbpC* are mainly involved in cell stability, and the number is four and nine for 35 and 70 mM W, respectively (Fig. 6, Table S5). The two-component system comprises of tetrathionate respiration (*ttrABC*), multidrug efflux system (*mdtABC* and *acrD*), envelope stress response (*zraPSR*), and hexose phosphate uptake (*uhpC* and *uhpT*) (Fig. 6, Table S5). As for the sulfur relay system, nine genes including *moaABCDE* and *tusACDE* were induced by 35 mM W and five genes were induced by 70 mM (Fig. 6, Table S5). Genes linked to bacterial secretion systems, T6SS, are *vgrG*, *hcp*, *lip,* and *clpV* (Fig. 6, Table S5). The enrichment results of differentially expressed genes were similar between 35 and 70 mM.

4. Discussion

4.1. Extracellular barrier and bioaccumulation

Citrobacter sp. Lzp2 could bioaccumulate large amounts of W on cell surfaces (Fig. 2 A). The sorption mechanism inferred by FTIR was that carboxyls bound W primarily (Fig. 2B). These carboxylic functional groups are likely in amino acids of proteins since our EPS composition analysis showed increased protein secretion in the presence of W (Fig. 1 F). A previous study also proposed the important role of carboxyl in adsorption of W on heat-treated *Escherichia coli* [40]. In addition, RNA-Seq results showed that four genes, *vgrG*, *hcp*, *lip,* and *clpV*, were significantly upregulated under W stress (Fig. 6 and Table S5). These four genes belong to the type VI secretory system (T6SS), which is a large molecule secretion device widely existed in gram-negative bacteria involved in the uptake of metal ions [41] and response to environmental stress [42]. The expression T6SS from *Yersinia pseudotuberculosis* can regulate zinc transportation via a novel Zn-binding protein, and rescue the sensitivity to oxidative stress [43]. Therefore, exposure to elevated W concentration can stimulate the T6SS system in *Citrobacter* sp. Lzp2, which enhances the production of extracellular proteins to chelate/-complex W anions outside cells.

RNA-Seq results indicated that the expression of *modA* was significantly downregulated (FDR<0.05, $|\log_2 FC = \geq 1$) (Table S5). W has specific ATP-binding cassette (ABC) transport system *tupABC* [44] and *wtpABC* [45], but they were not annotated in reference genomes of *Citrobacter* sp.). In addition, W can be transferred into cells through the Mo ABC transport system (*modABC)* [46]. Thus, downregulated *modA* enables *Citrobacter* sp. Lzp2 maintains W homeostasis to prevent metal overload.

4.2. Intracellular storage and detoxification

The intracellular W concentration reached > 0.5 mmol/g in *Citrobacter* sp. Lzp2 cells when exposed to 35–110 mM W, showing their high intracellular accumulation capacity (Fig. 2A). Generally speaking, when there is an influx of metals, temporary sequestration of metals in a storage protein allows the uptake systems to be repressed and the efflux

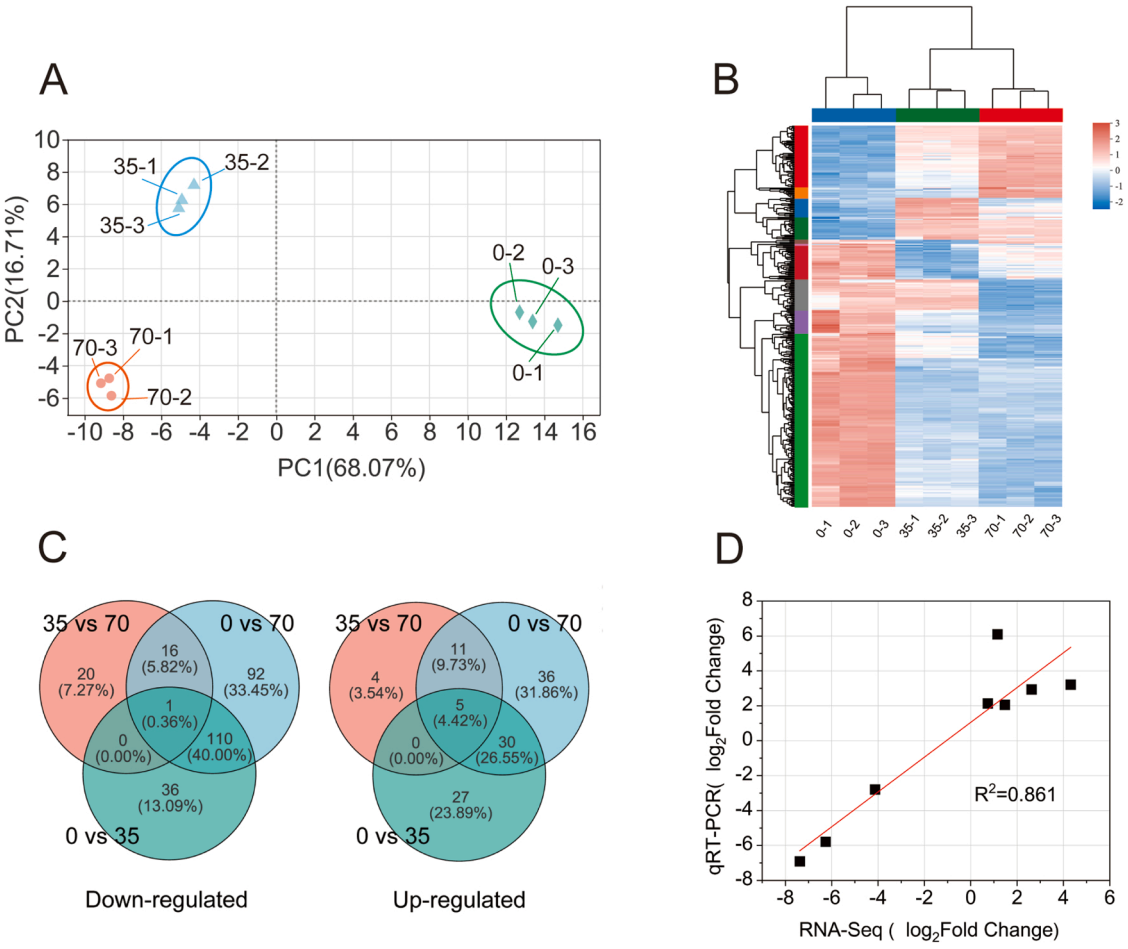

Fig. 3. Distribution of differentially expressed genes and qRT-PCR validation. A. Principal component analysis of all individual samples: 0 mM W, green; 35 mM W, blue; 70 mM W, red. B. Heatmap illustrating expression levels of all differentially regulated transcripts in all individual samples. C. Venn diagram showing the common and unique upregulated or downregulated expressed genes. The percentages mean the ratio of numbers of differentially expressed genes (0 vs 35, 0 vs 70, and 35 vs 70 mM) to all upregulated genes or downregulated genes. D. Correlation between RNA-Seq and qRT-PCR for the eight selected genes. The results showed a significant correlation ($R^2 = 0.861$; $p < 0.001$) between the RNA-Seq and qRT-PCR data.

systems to be activated [20]. Prominent among these W-storage or -sequestration proteins can be divided into two categories. Firstly, according to our GO and KEGG enrichment results, *ibpAB*, *dnaJK,* and *cpxP* linked to protein and anion binding (GO terms), and *zraSRP* associated with the two-component system (KEGG pathway), were upregulated significantly (Figs. 4–6, and Table S5). These genes regulate the expression of chaperone proteins that serve for envelope repair (*zraSRP* and *cpxP*) and protein homeostasis (*ibpAB* and *dnaJK*) [47-49]. Periplasmic chaperone protein ZraP can also directly bind toxic metals such as copper and zinc [50]. Hence, chaperone proteins play a role not only in cell stability but also in functioning as a chelator to bind W for homeostasis. Secondly, the sulfur relay system regulates the synthesis of molybdopterin. Activation of this metabolic system was observed both at 35 mM W (p-adj<0.05) and 70 mM W (uncorrected $p < 0.05$) (Figs. 5 and 6, and Table S5). Mo is indispensable for the formation of many enzymes such as nitrogenase, nitrate reductases, and sulfite oxidase [51]. Mo is integrated into cofactors through complex biosynthetic pathways as the catalytic center [52]. A preview study found that some molybdoenzymes could remain active after W substitution [53]. Accordingly, the cytoplasmic W in *Citrobacter* sp. Lzp2 may substitute Mo to participate in the synthetic process of the metal-binding pterin (MPT), tungstopterin [54]. Another role of the sulfur relay system is to form 2-thiouridylation of 5-methylaminomethyl-2-thiouridine (mnm^5s^2U) [55], which controls phosphate homeostasis to regulate metabolic state [56]. Admittedly, other cellular buffering proteins and macromolecules may present, such as amino acid, glutathione, organic acid, and inorganic ligand. They, together with these specific storage proteins, collectively regulate cell W homeostasis and provide a window of opportunity for cells to express other proteins to facilitate adaptation to excess W.

Notably, *ttrABC* genes for tetrathionate respiration attached to the two-component system were upregulated significantly in both 35 and 70 mM W treatments (Fig. 5, and Table S5). This respiration occurs in certain genera of *Enterobacteriaceae* including *Salmonella*, *Citrobacter,* and *Proteus*, which allows bacteria to make use of tetrathionate for metabolism under various conditions [57]. Ttr could catalyze tetrathionate ($-O_3S-S-SO_3-$) to two molecules of thiosulphate ($-S-SO_3-$) (Hensel et al., 1999). In anaerobic aquifers, W can form thio-tungstate with inorganic sulfate under sulfate reduction [58], which greatly affects the solubility and transport of W [59]. The formed cytosolic $2-S-SO_3-$ could bind W to produce such thio-tungstate via the W–S bonds. In contrast to the general knowledge that tetrathionate respiration is more prevalent under anaerobic conditions [60,61], our results implied that W stress could activate bacterial tetrathionate respiration in an aerobic environment. *Citrobacter* sp. Lzp2 probably binds W for maintaining homeostasis and detoxification through this special tetrathionate metabolic pathway, which has never been reported previously.

Another detoxification mechanism is linked to the raising of environmental pH. The pH of the culture medium increased from ~7 to > 8 (Fig. S4). Polymeric tungstates, which are easier to form under lower pH

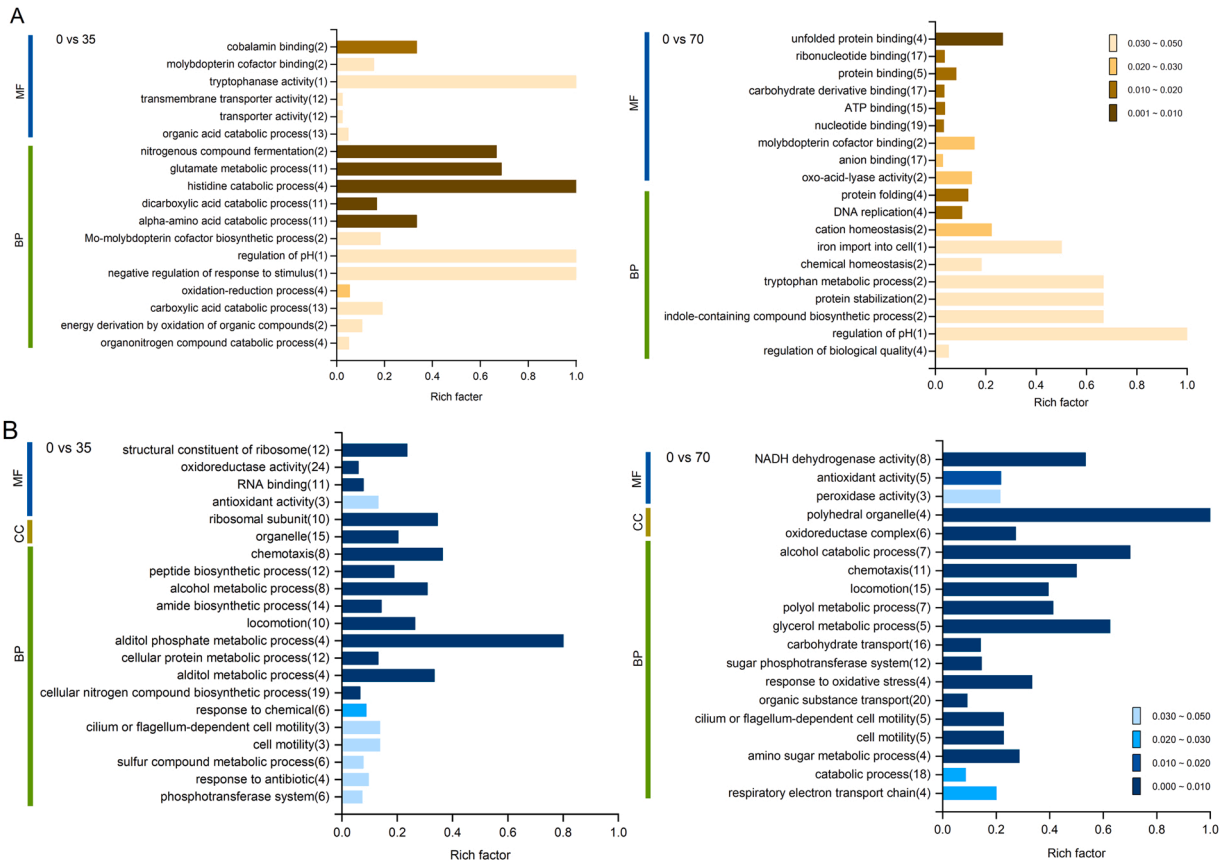

Fig. 4. GO functional enrichment histogram of Citrobacter sp. Lzp2 exposing to 35 mM and 70 mM W, showing the enriched terms of (A) up-regulated and (B) down-regulated genes. Names of GO terms including the gene number in brackets are listed along the y-axis. The enrichment factor (x-axis) represents the numbers of differentially expressed genes annotated in a particular pathway term to the numbers of all genes annotated in this pathway. P-adj ranged from 0 to 0.05, with a p-adj closer to 0 indicating greater enrichment.

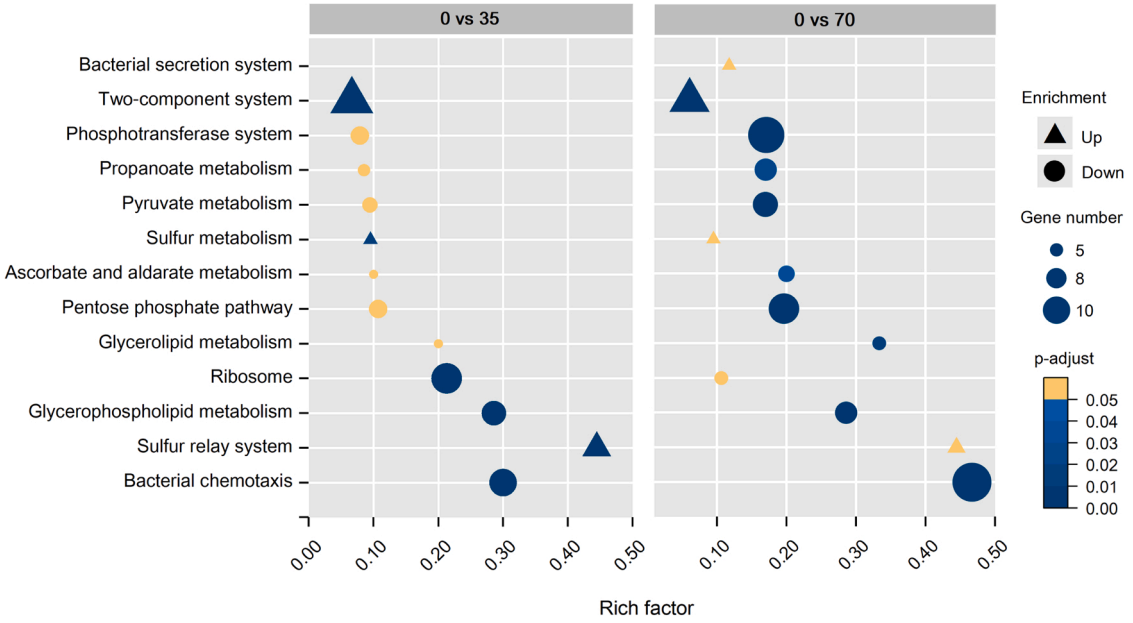

Fig. 5. Enrichment scatters diagram of KEGG pathways in *Citrobacter* sp. Lzp2 exposing to 35 mM and 70 mM W compared with the control. Names of KEGG pathways are listed along the y-axis. The enrichment factor (*x*-axis) represents the numbers of differentially expressed genes annotated in a particular pathway term to the numbers of all genes annotated in this pathway. *P*-adj range from 0 to 0.05, with a *p*-adj closer to 0 indicating greater enrichment. The yellow ones represent the *p*-adiust> 0.05 and *p*-uncorrected< 0.05 KEGG pathways.

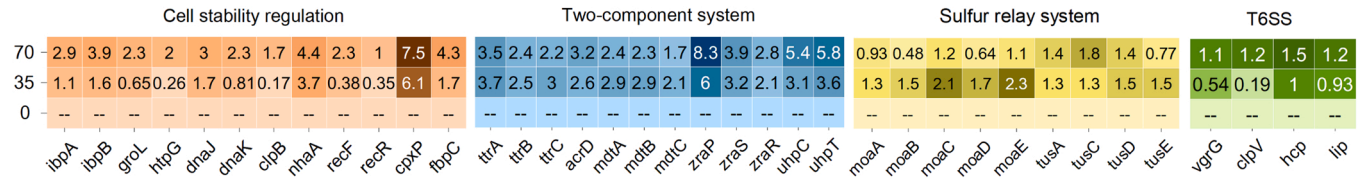

Fig. 6. The expression level (Log_2FC) of DEGs assigned to protein binding and cell stability regulation, two-component system, sulfur relay system, and bacterial secretion system (T6SS) in RNA-seq of *Citrobacter* sp. Lzp2 under 35 mM and 70 mM W stress.

[62], are more toxic to organisms than mono-meric tungstates [1]. RNA-Seq showed that the regulation of pH terms were upregulated significantly at both W treatments (Fig. 4 A), besides, amino acid metabolism (histidine catabolic process, glutamate metabolism, dicarboxylic acid catabolic process, and alpha-amino acid catabolic process) increased significantly at 35 mM W (Fig. 4 A). Increased metabolism of amino acids could elevate pH by producing ammonia ($NH_3 + H_2O \rightleftharpoons NH_4^+ + OH^-$) [63]. These metabolism processes prevent the formation of polymeric tungstates to make W less toxic.

4.3. Efflux system

SEM results showed that the cell size of *Citrobacter* sp. Lzp2 became smaller in the presence of W (Fig. 1B-E). This size decrease may be partially caused by excretion of W outside cells accompanied by cytoplasmic lysis [64,65]. In addition, transcriptional results showed that genes belonging to multiple drug efflux pumps (BaeSR system) were significantly upregulated in 35 mM W treatment (*mdtABC* and *acrD*) and 70 mM treatment (*mdtABCD*, *baeS* and *acrD*) (Fig. 6 and Table S5). Meanwhile, physiological results illustrated that extracellular biosorption was greater than intracellular bioaccumulation (Fig. 2 A). The BaeSR system is a two-component signal transduction pathway, regulating *arcD, syp* genes, and *mdtABCD-baeSR* operon which are involved in envelope stress response, drug resistance, and metal resistance [24, 66]. Leblanc et al. [24] indicated that sodium tungstate is an inducer of the BaeSR response and a natural substrate of the *MdtABC* efflux pump. Combined with previous findings, our results showed that this efflux system (BaeSR system) is important for the homeostasis of W in *Citrobacter* sp. Lzp2.

4.4. Multiple resistance mechanisms of Citrobacter sp. Lzp2 to W stress

Based on the physiologic and RNA-Seq results, we delineate a relatively clear profile of the multiple resistance mechanisms (Fig. 7): 1) Upregulated T6SS secretes more extracellular proteins to complex/chelate W via the carboxylic functional groups; 2) Downregulated *modA* reduces W transport into cells, and multi-drug efflux system (Mdt and AcrD) excretes cytosolic W outside cells; 3) Sulfur relay system, tetrathionate respiration (Ttr) and raising pH by amino acid metabolism involve in cytosolic W storage and detoxification, providing enough time for the W uptake systems to be repressed and W efflux or sequestration systems to be activated; 4) Chaperone proteins in the periplasm and cytoplasm (ZraSRP, IbpAB, DnaJK, and CpxP) participate in cell stability regulation, and ZraP may also directly bind W to protect cells against W poisoning.

5. Conclusions

This study suggests a high-tolerance and positive response of *Citrobacter* sp. Lzp2 to W-enriched condition and multiple transcriptional pathways collectively mediate W resistance. Our results built a comprehensive view of the W-resistance mechanisms of bacteria, especially identifying the specific W response gene clusters, which are of great importance for understanding W homeostasis in prokaryotes. Admittedly, given the diversity of bacteria in nature, whether they have evolved other strategies to reducing W toxicity awaits further experimental validation of different bacterial species. Microbial tungstenproteomes are still largely uncharacterized, and the potential for discovering novel metalloregulatory proteins is promising. Another new and exciting frontier is in the bio-extraction of recovery of W from

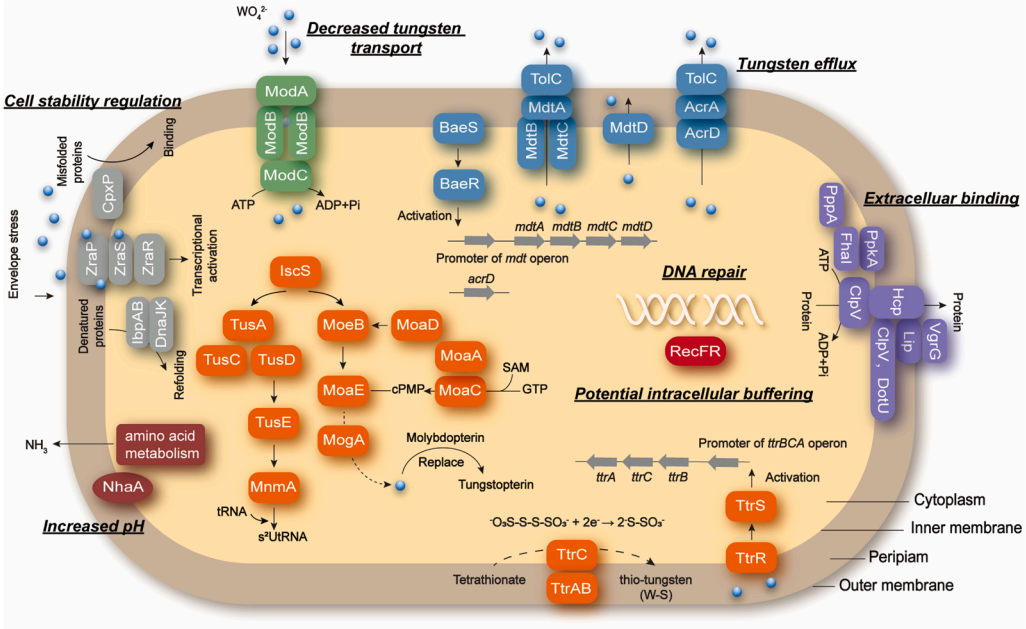

Fig. 7. Conceptual metabolic model for W-resistant mechanisms of *Citrobacter* sp. Lzp2. The colored texts indicate significantly upregulated genes or pathways under W stress: cell stability regulation genes (gray), multiple drug efflux systems (Mdt and AcrD) (blue), amino acid metabolism (dark red), potential intracellular detoxification pathways including sulfur relay system and tetrathionate respiration (orange), DNA repair genes (red), Type VI secretion system (dark blue) and Mo transport system (green).

wastewaters. Given the high tolerance and bioaccumulation characteristics (up to 3.4 mmol/g cells), *Citrobacter* sp. Lzp2 may assist novel extraction and recovery processes of W, which is of great significance to the recovery of strategic metals. *Citrobacter* sp. Lzp2 can also be used as a bio-remediation technology to treat W-contaminated soils and sediments.

Environmental Implication

Tungsten (W) was found to be much more toxic than previously recognized, making it an emerging contaminant and creating a need for research into its toxicology to the biosphere. Here, we built a first W-resistance profile of the bacterium, Citrobacter sp. Lzp2, screened from W-contaminated soil. We found several potential new metabolic pathways for W detoxification such as the tetrathionate respiration, and multiple transcriptional pathways collectively mediate W resistance. The results of this study have implications for understanding the intricate regulatory network of W homeostasis in microbes, as well as future bio-recovery and bioremediation of W in contaminated environmental systems.

CRediT authorship contribution statement

Zipei Luo: Methodology, Software, Formal analysis, Investigation, Visualization, Writing – original draft; **Zhen Li**: Writing – review & editing; **Jing Sun**: Writing – review & editing; **Kaixiang Shi**: Writing – review & editing; **Ming Lei**: Supervision; **Boqing Tie**: Supervision; **Huihui Du**: Conceptualization, Methodology, Software, Resources, Data curation, Writing – review & editing, Visualization, Project administration, Funding acquisition.

Declaration of Competing Interest

The authors declare the following financial interests/personal relationships which may be considered as potential competing interests: Huihui Du reports financial support was provided by National Natural Science Foundation of China.

Data Availability

Data will be made available on request.

Acknowledgments

This work was financially supported by the National Natural Science Foundation of China (NSFC, No. 41907015). We acknowledge Shanghai Majorbio Bio-pharm Technology Co., Ltd for genome sequencing and analysis, and Hangzhou Lianchuan Biotechnology Co., Ltd for 16S rRNA analysis.

Appendix A. Supporting information

Supplementary data associated with this article can be found in the online version at doi:10.1016/j.jhazmat.2023.130877.

References

[1] Koutsospyros, A., Braida, W., Christodoulatos, C., Dermatas, D., Strigul, N., 2006. A review of tungsten: from environmental obscurity to scrutiny. J Hazard Mater 136, 1–19.
[2] Xu, Z., Liu, X., Peng, J., Qu, C., Chen, Y., Zhang, M., et al., 2022. Tungsten–humic substances complexation. Carbon Res 1, 11.
[4] Du, H., Liu, X., Li, Y., Luo, Z., Lei, M., Tie, B., 2021. A review on the environmental behavior and potential risk of tungsten in soils: Progress and prospects. Acta Pedol Sin 654–665.
[3] Bostick, B.C., Sun, J., Landis, J.D., Clausen, J.L., 2018. Tungsten speciation and solubility in munitions-impacted soils. Environ Sci Technol 52, 1045–1053.
[5] Hobson, C., Kulkarni, H., Johannesson, K., Bednar, A., Tappero, R., Mohajerin, T.J., 2020. Origin of tungsten and geochemical controls on its occurrence and mobilization in shallow sediments from Fallon, Nevada, USA. Chemosphere, 127577.
[6] Sheppard, P.R., Ridenour, G., Speakman, R.J., Witten, M.L., 2006. Elevated tungsten and cobalt in airborne particulates in Fallon, Nevada: Possible implications for the childhood leukemia cluster. Appl Geochem 21, 152–165.
[8] Steenstra, P., Strigul, N., Harrison, J., 2020. Tungsten in Washington state surface waters. Chemosphere 242, 125151.
[7] Cidu, R., Biddau, R., Frau, F., Wanty, R.B., Naitza, S., 2021. Regional occurrence of aqueous tungsten and relations with antimony, arsenic and molybdenum concentrations (Sardinia, Italy). J Geochem Explor 229, 106846.
[9] Seiler, R.L., Stollenwerk, K.G., Garbarino, J.R., 2005. Factors controlling tungsten concentrations in ground water, Carson Desert, Nevada. Appl Geochem 20, 423–441.
[10] Adamakis, I.-D.S., Eleftheriou, E.P., Rost, T.L., 2008. Effects of sodium tungstate on the ultrastructure and growth of pea (Pisum sativum) and cotton (Gossypium hirsutum) seedlings. Environ Exp Bot 63, 416–425.
[11] Ringelberg, D., Reynolds, C., Winfield, L., Inouye, L., Johnson, D., Bednar, A., 2009. Tungsten effects on microbial community structure and activity in a soil. J Environ Qual 38, 103–110.
[12] Inouye, L.S., Jones, R.P., Bednar, A.J., 2006. Tungsten effects on survival, growth, and reproduction in the earthworm, *Eisenia fetida*. Environ Toxicol Chem 25, 763–768.
[13] Rubin, C.S., Holmes, A.K., Belson, M.G., Jones, R.L., Flanders, W.D., Kieszak, S.M., 2007. Investigating childhood leukemia in Churchill County, Nevada. Environ Health Perspect 115, 151–157.
[14] The united state environmental protection agency. (accessed April 2008) Emerging Contaminant-Tungsten. https://www.epa.gov/fedfac/technical-fact-sheettungsten.
[15] Harrison, J.J., Ceri, H., Turner, R.J., 2007. Multimetal resistance and tolerance in microbial biofilms. Nat Rev Micro 5, 928–938.
[16] Lemire, J.A., Harrison, J.J., Turner, R.J., 2013. Antimicrobial activity of metals: mechanisms, molecular targets and applications. Nat Rev Microbiol 11, 371–384.
[17] Wichard, T., Bellenger, J.-P., Loison, A., Kraepiel, A.M., 2008. Catechol siderophores control tungsten uptake and toxicity in the nitrogen-fixing bacterium *Azotobacter vinelandii*. Environ Sci Technol 42, 2408–2413.
[18] Strigul, N., Koutsospyros, A., Arienti, P., Christodoulatos, C., Dermatas, D., Braida, W., 2005. Effects of tungsten on environmental systems. Chemosphere 61, 248–258.
[19] Sugio, T., Kuwano, H., Negishi, A., Maeda, T., Takeuchi, F., Kamimura, K., 2001. Mechanism of growth inhibition by tungsten in *Acidithiobacillus ferrooxidans*. Biosci Biotechnol Biochem 65, 555–562.
[21] Silver, S., Phung, L.T., 1996. Bacterial heavy metal resistance: new surprises. Annu Rev Microbiol 50, 753–789.
[20] Chandrangsu, P., Rensing, C., Helmann, J., 2017. Metal homeostasis and resistance in bacteria. Nat Rev Microbiol 15, 338–350.
[22] Wang, M., Ma, J., Wang, X., Wang, Z., Tang, L., Chen, H., et al., 2020. Detoxification of Cu(II) by the red yeast *Rhodotorula mucilaginosa*: from extracellular to intracellular. Appl Microbiol Biotechnol 104, 10181–10190.
[23] Wang, Z., Zhang, Y., Jiang, L., Qiu, J., Gao, Y., Gu, T., et al., 2022. Responses of Rhodotorula mucilaginosa under Pb(II) stress: carotenoid production and budding. Environ Microbiol 24, 678–688.
[24] Leblanc, S.K., Oates, C.W., Raivio, T.L., 2011. Characterization of the induction and cellular role of the BaeSR two-component envelope stress response of *Escherichia coli*. J Bacteriol 193, 3367–3375.
[25] Kazakov, A.E., Rajeev, L., Luning, E.G., Zane, G.M., Siddartha, K., Rodionov, D.A., 2013. New family of tungstate-responsive transcriptional regulators in sulfate-reducing bacteria. J Bacteriol 195, 4466–4475.
[26] Huang, N., Mao, J., Zhao, Y., Hu, M., Wang, X., 2019. Multiple transcriptional mechanisms collectively mediate copper resistance in *Cupriavidus gilardii* CR3. Environ Sci Technol 53 (4609–4618).
[27] Li, L.J., Lin, Q., Li, T.Z., He, X.H., Peng, S.M., Tao, Y., 2020. Transcriptional response of *Pseudomonas chenduensis* strain MBR to cadmium toxicity. Appl Microbiol Biotechnol 104, 9749–9757.
[28] Matyar, F., 2012. Antibiotic and heavy metal resistance in bacteria isolated from the eastern mediterranean sea coast. Bull Environ Contam Toxicol 89, 551–556.
[29] Parisa, K., Mehran, H., Arezoo, T., 2011. Multi-metal resistance study of bacteria highly resistant to mercury isolated from dental clinic effluent. Afr J Microbiol Res 5 (7), 831–837.
[30] Du, H., Li, Y., Wan, D., Sun, C.Q., Sun, J., 2022. Tungsten distribution and vertical migration in soils near a typical abandoned tungsten smelter. J Hazard Mater 429, 128292.
[31] Teng, Z., Shao, W., Zhang, K., Huo, Y., Zhu, J., Li, M., 2019. Pb biosorption by *Leclercia adecarboxylata*: Protective and immobilized mechanisms of extracellular polymeric substances. Chem Eng J 375, 122113.
[32] Raunkjær, K., Hvitved-Jacobsen, T., Nielsen, P.H., 1994. Measurement of pools of protein, carbohydrate and lipid in domestic wastewater. Water Res 28, 251–262.
[33] Bradford, M.M., 1976. A rapid and sensitive method for the quantitation of microgram quantities of protein utilizing the principle of protein-dye binding. Anal Biochem 72, 248–254.
[34] Shi, Y., Wang, Y., Wang, D., Liu, B., Li, Y., Wei, L., 2012. Synthesis of hexagonal prism (La, Ce, Tb) PO_4 phosphors by precipitation method. Cryst Growth Des 12, 1785–1791.

[35] Fang, L., Zhou, C., Cai, P., Chen, W., Rong, X., Dai, K., 2011. Binding characteristics of copper and cadmium by *Cyanobacterium Spirulina platensis*. J Hazard Mater 190, 810–815.
[36] Su, S., Zeng, X., Bai, L., Jiang, X., Li, L., 2010. Bioaccumulation and biovolatilisation of pentavalent arsenic by *Penicillin janthinellum*, *Fusarium oxysporum* and *Trichoderma asperellum* under laboratory conditions. Curr Microbiol 61, 261–266.
[37] Gustafsson, J.P., 2003. Modelling molybdate and tungstate adsorption to ferrihydrite. Chem Geol 200, 105–115.
[38] Livak, K.J., Schmittgen, T.D., 2001. Analysis of relative gene expression data using real-time quantitative PCR and the $2^{-\Delta\Delta CT}$ method. Methods 25, 402–408.
[39] Rakshit, S., Sallman, B., Davantés, A., Lefèvre, G., 2017. Tungstate (VI) sorption on hematite: An in situ ATR-FTIR probe on the mechanism. Chemosphere 168, 685–691.
[40] Ogi, T., Sakamoto, Y., Nandiyanto, A.B.D., Okuyama, K., 2013. Biosorption of tungsten by *Escherichia coli* for an environmentally friendly recycling system. Ind Eng Chem Res 52, 14441–14448.
[41] Coulthurst, S., 2019. The Type VI secretion system: a versatile bacterial weapon. Microbiology 165, 503–515.
[42] Weber, B., Hasic, M., Chen, C., Wai, S.N., Milton, D.L., 2009. Type VI secretion modulates quorum sensing and stress response in *Vibrio anguillarum*. Environ Microbiol 11, 3018–3028.
[43] Wang, T., Si, M., Song, Y., Zhu, W., Gao, F., Wang, Y., 2015. Type VI secretion system transports Zn^{2+} to combat multiple stresses and host immunity. PLoS Pathog 11, e1005020.
[44] Makdessi, K., Andreesen, J.R., Pich, A., 2001. Tungstate uptake by a highly specific ABC transporter in *Eubacterium acidaminophilum*. J Biol Chem 276, 24557–24564.
[45] Bevers, L.E., Hagedoorn, P.-L., Krijger, G.C., Hagen, W.R., 2006. Tungsten transport protein A (WtpA) in *Pyrococcus furiosus*: the first member of a new class of tungstate and molybdate transporters. J Bacteriol 188, 6498–6505.
[46] Tejada-Jiménez, M., Llamas, Á., Sanz-Luque, E., Galván, A., Fernández, E., 2007. A high-affinity molybdate transporter in eukaryotes. Proc Natl Acad Sci USA 104, 20126–20130.
[47] Hunke, S., Keller, R., Muller, V.S., 2012. Signal integration by the Cpx-envelope stress system. FEMS Microbiol Lett 326, 12–22.
[48] Mogk, A., Ruger-Herreros, C., Bukau, B., 2019. Cellular functions and mechanisms of action of small heat shock proteins. Annu Rev Microbiol 73, 89–110.
[49] Rome, K., Borde, C., Taher, R., Cayron, J., Lesterlin, C., Gueguen, E., 2018. The two-component system ZraPSR is a novel ESR that contributes to intrinsic antibiotic tolerance in *Escherichia coli*. J Mol Biol 430, 4971–4985.
[50] Petit-Hartlein, I., Rome, K., de Rosny, E., Molton, F., Duboc, C., Gueguen, E., 2015. Biophysical and physiological characterization of ZraP from *Escherichia coli*, the periplasmic accessory protein of the atypical ZraSR two-component system. Biochem J 472, 205–216.
[51] Schwarz, G., Mendel, R.R., Ribbe, M.W., 2009. Molybdenum cofactors, enzymes and pathways. Nature 460, 839–847.
[52] Schwarz, G., 2005. Molybdenum cofactor biosynthesis and deficiency. Cell Mol Life Sci 62, 2792–2810.
[53] Buc, J., Santini, C.L., Giordani, R., Czjzek, M., Wu, L.F., Giordano, G., 1999. Enzymatic and physiological properties of the tungsten-substituted molybdenum TMAO reductase from *Escherichia coli*. Mol Microbiol 32, 159–168.
[54] McMaster, J., Enemark, J.H., 1998. The active sites of molybdenum-and tungsten-containing enzymes. Curr Opin Chem Biol 2, 201–207.
[55] Ikeuchi, Y., Shigi, N., Kato, J., Nishimura, A., Suzuki, T., 2006. Mechanistic insights into sulfur relay by multiple sulfur mediators involved in thiouridine biosynthesis at tRNA wobble positions. Mol Cell 21, 97–108.
[56] Gupta, R., Walvekar, A.S., Liang, S., Rashida, Z., Shah, P., Laxman, S., 2019. A tRNA modification balances carbon and nitrogen metabolism by regulating phosphate homeostasis. Elife 8, e44795.
[57] de Pina, L.C., da Silva, F.S.H., Galvao, T.C., Pauer, H., Ferreira, R.B.R., Antunes, L. C.M., 2021. The role of two-component regulatory systems in environmental sensing and virulence in *Salmonella*. Crit Rev Microbiol 47, 397–434.
[58] Mohajerin, T.J., Helz, G.R., White, C.D., Johannesson, K.H., 2014. Tungsten speciation in sulfidic waters: Determination of thiotungstate formation constants and modeling their distribution in natural waters. Geochim Cosmochim Acta 144, 157–172.
[59] Johannesson, K.H., Dave, H.B., Mohajerin, T.J., Datta, S., 2013. Controls on tungsten concentrations in groundwater flow systems: The role of adsorption, aquifer sediment Fe (III) oxide/oxyhydroxide content, and thiotungstate formation. Chem Geol 351, 76–94.
[61] Price-Carter, M., Tingey, J., Bobik, T.A., Roth, J.R., 2001. The alternative electron acceptor tetrathionate supports B12-dependent anaerobic growth of *Salmonella enterica* serovar Typhimurium on ethanolamine or 1, 2-propanediol. J Biotechnol 183, 2463–2475.
[60] Daeffler, K.N., Galley, J.D., Sheth, R.U., Ortiz-Velez, L.C., Bibb, C.O., Shroyer, N.F., 2017. Engineering bacterial thiosulfate and tetrathionate sensors for detecting gut inflammation. Mol Syst Biol 13, 923.
[62] Strigul, N., Koutsospyros, A., Christodoulatos, C., 2010. Tungsten speciation and toxicity: acute toxicity of mono-and poly-tungstates to fish. Ecotoxicol Environ Saf 73, 164–171.
[63] Huang, S., Liu, R., Sun, M., Li, X., Guan, Y., Lian, B., 2022. Transcriptome expression analysis of the gene regulation mechanism of bacterial mineralization tolerance to high concentrations of Cd^{2+}. Sci Total Environ 806, 150911.
[64] Lancaster, W.A., Menon, A.L., Scott, I., Poole, F.L., Vaccaro, B.J., Thorgersen, M.P., 2014. Metallomics of two microorganisms relevant to heavy metal bioremediation reveal fundamental differences in metal assimilation and utilization. Metallomics 6, 1004–1013.
[65] Ngwenya, B.T., 2007. Enhanced adsorption of zinc is associated with aging and lysis of bacterial cells in batch incubations. Chemosphere 67, 1982–1992.
[66] Wang, D., Fierke, C.A., 2013. The BaeSR regulon is involved in defense against zinc toxicity in *E. coli*. Metallomics 5, 372–383.